LU TP 13-32
September 2013

Search for technipions in exclusive production of diphotons with large invariant masses at the LHC

Piotr Lebiedowicz,[1,*] Roman Pasechnik,[2,†] and Antoni Szczurek[3,4,‡]

[1] *Institute of Nuclear Physics PAN, PL-31-342 Cracow, Poland*
[2] *Department of Astronomy and Theoretical Physics, Lund University, SE-223 62 Lund, Sweden*
[3] *University of Rzeszów, PL-35-959 Rzeszów, Poland*
[4] *Institute of Nuclear Physics PAN, PL-31-342 Cracow, Poland*

Abstract

We focus on exclusive production of neutral technipion $\tilde{\pi}^0$ in pp collisions at the LHC, i.e. on $pp \to pp\tilde{\pi}^0$ reaction. The dependence of the cross section on parameters of recently proposed vector-like Technicolor model is studied. Characteristic features of the differential distributions are discussed. For not too large technipion masses the diphoton decay channel has the dominant branching fraction. This is also the main reason for an enhanced production of neutral technipions in $\gamma\gamma$-fusion reaction. We discuss potential backgrounds of the QCD and QED origin to the $pp \to pp(\tilde{\pi}^0 \to \gamma\gamma)$ process at large invariant $\gamma\gamma$ masses. We conclude that compared to inclusive case the signal-to-background ratio in the considered exclusive reaction is vary favorable which thereby could serve as a good probe for Technicolor dynamics searches at the LHC.

PACS numbers: 14.80.Ec, 14.80.Bn, 12.60.Nz, 14.80.Tt, 12.60.Fr

*Electronic address: Piotr.Lebiedowicz@ifj.edu.pl
†Electronic address: Roman.Pasechnik@thep.lu.se
‡Electronic address: Antoni.Szczurek@ifj.edu.pl

I. INTRODUCTION

A typical central exclusive production (CEP) process with the signature $pp \to p + X + p$, where X is a diffractive system separated from the two very forward protons by large rapidity gaps, is considered to be very sensitive to New Physics contributions. In particular, it has been proposed as an alternative way of searching for neutral Higgs bosons and SUSY particles (see Ref. [1, 2] for a review on the topic) due to a reduced QCD $b\bar{b}$ background. In this paper, we would like to focus on an extra interesting opportunity of making use of large rapidity gap processes at the LHC for probing new strongly-coupled dynamics.

For the QCD-initiated CEP processes there is a serious problem of rather large theoretical uncertainties of the QCD diffraction mechanism in the framework of the Durham Model (see e.g. Ref. [3]). These uncertainties come from both the hard subprocess treatment and soft $k_\perp$-dependent parton densities as well as from a model-dependent gap survival probability factor (see e.g. Refs. [4–7]). This situation forces the search for various possible ways to probe the underlying CEP QCD mechanism. In order to reduce theoretical uncertainties, new experimental data on various exclusive production channels are certainly required and expected to come soon from ongoing LHC measurements. In particular, a measurement of the exclusive dijets production at the LHC could largely reduce the theoretical uncertainty in the Higgs boson CEP [4]. Other measurements of exclusive heavy quarkonia [6, 7], $\gamma\gamma$ [7] and W^+W^- pairs [8], high-$p_\perp$ light mesons [9, 10], exclusive associated charged Higgs H^+W^- [11] CEP, etc., can also be important in this context.

Besides the QCD-initiated CEP processes like the exclusive Higgs and dijet production, there are extra QED-initiated contributions coming from $\gamma\gamma \to X$ subprocesses. Normally, these contributions are strongly suppressed by very small fine structure constant and therefore typically neglected compared to the QCD ones especially for not very large invariant X-system masses, except for leading-order exclusive dilepton $X \equiv l^+l^-$ production. On the other hand, the exclusive reaction via the $\gamma\gamma$ fusion have significantly smaller theoretical uncertainties compared to the QCD-initiated Durham mechanism making it a very appealing option for New Physics searches for exotic resonances which are coupled to photons or SM gauge bosons only.

Recently, the CMS Collaboration has indicated yet unexplained resonant 2σ-signature in the $\gamma\gamma$ invariant mass spectrum around ~ 137 GeV [12]. Regardless of whether this is physical or not it is worth to search for simplest possibilities of having an extra narrow neutral resonance decaying predominantly into the $\gamma\gamma$ pair. These exotic light physical states, such as technipions, are naturally predicted by a high-scale strongly-coupled dynamics commonly referred to as Technicolor (TC) [13, 14] (for a review, see also Ref. [15, 16]).

In original minimal Higgs-less TC models, the EW symmetry is broken by techniquark condensate $\langle Q\bar{Q}\rangle$ and there are no composite scalars left in the spectrum since pseudo-Goldstone technipions appearing due to the chiral symmetry breaking at a TeV energy scale are absorbed by the SM gauge bosons. Recently, however, the SM Higgs boson has been discovered [17, 18] leaving practically no room for minimal TC scenarios, and the search for consistent alternatives incorporating new strongly-coupled dynamics, dynamical EW symmetry breaking (EWSB) and the (elementary or composite) Higgs boson is on the way.

Many existing dynamical EWSB scenarios, including those with walking and topcolor dynamics, incorporate more than the minimal two flavors of techniquarks. Such scenarios feature pseudo-scalar technipion states that are remnants of the EWSB in models with more than one weak techniquark doublet. Discovery of such technipions is often considered as one

the basic observational signatures of TC [20–22]. In extended TC scenarios with colorless (or colored) techniquarks the technipion can be produced via gluon-gluon and quark-antiquark fusion through a strong technipion coupling to heavy t, b quarks (or techniquark-gluon coupling). As was shown in Ref. [19] (and in references therein) in such scenarios the relatively light technipions $m_{\tilde{\pi}} < 2m_t$ are excluded by the SM Higgs searches at the LHC. Do we still have a room for light ($m_{\tilde{\pi}} \sim 100 - 300$ GeV) technipions consistent with EW and LHC precision constraints?

In this paper, we consider an alternative realization of the dynamical EWSB ideas – the so-called vector-like TC scenario recently proposed and discussed in detail in Refs. [23, 24]. This model is a successful alternative to the standard (Extended, Walking) TC implementations which is essentially the minimal TC extension of the SM with one (elementary or composite) Higgs doublet and extra strongly-coupled weak doublet of vector-like techniquarks (i.e. with two "techni-up" U and "techni-down" D flavors only).

The idea of vector-like (chiral-symmetric) ultraviolet completion which is fully consistent with precision EW constraints at the fundamental level has been realized in the framework of the gauged linear σ-model initially developed for QCD hadron physics [25–27]. In this phenomenological approach, the spontaneous *global* chiral symmetry breaking in the techiquark sector happens by means of technisigma vacuum expectation value (vev) in the chiral-symmetric (vector-like) way

$$SU(2)_{\rm L} \otimes SU(2)_{\rm R} \to SU(2)_{\rm V\equiv L+R}\,, \tag{1.1}$$

where the resulting unbroken chiral-symmetric subgroup $SU(2)_{\rm V\equiv L+R}$ is then *gauged* and therefore describes gauge interactions of the techniquark sector. The minimality of such a scenario which incorporates the SM Higgs sector is provided by the fact that one gauges *only* the vector part of the global chiral symmetry. In Ref. [23] it was argued that the vector-like gauge group $SU(2)_{\rm V}$ can, in principle, be *identified* with the weak isospin group $SU(2)_{\rm W}$ of the SM, i.e.

$$SU(2)_{\rm V\equiv L+R} \equiv SU(2)_{\rm W}\,, \tag{1.2}$$

in the techniquark sector. Such a dynamical realization of the chiral-gauge symmetry leads to specific properties of the techniquark sector w.r.t. weak interactions, which thereby make it to be very different from the chiral-nonsymmetric SM fermion sectors. It therefore means that after the chiral symmetry breaking in the techniquark sector the left and right components of the original Dirac techniquark fields can interact with the SM weak $SU(2)_{\rm W}$ gauge bosons with vector-like couplings, in contrast to ordinary SM fermions, which interact under $SU(2)_{\rm W}$ by means of their left-handed components only.

The resulting weak isospin symmetry $SU(2)_{\rm W}$ is broken by means of the effective SM Higgs mechanism which thereby gets *initiated* by the techniquark condensation providing the dynamical nature of the EWSB [23]. In this scenario, the additional Goldstone bosons arising from the Higgs weak doublet are absorbed by $Z, W^{\pm}$ bosons in the standard way while pseudo-Goldstone technipions from extra TC dynamics remain physical in a full analogy with QCD hadron physics. As we will see below these technipions can be rather light, in principle, as light as the W boson since they do not couple to ordinary quarks and gluons and could potentially be accessible to a standard Higgs boson searches e.g. in $\gamma\gamma$ and γZ decay channels. Since the diphoton channel appears to be the most favorable channel for such technipion searches at the LHC we wish to discuss in the present paper also the

diphoton backgrounds which turn out to be suppressed compared to the $\tilde{\pi}^0 \to \gamma\gamma$ signal in the exclusive production process.

In this paper, we therefore consider the exclusive production of $\gamma\gamma$ pairs which is among one of the diffractive "golden channels" for both Higgs boson and light technipion searches at the LHC. The $pp \to p(\gamma\gamma)p$ process going through the diffractive QCD mechanism with the $gg \to \gamma\gamma$ subprocess naturally constitutes a background for the resonant technipion production. The photon-photon contribution for the purely exclusive production of low invariant mass of $\gamma\gamma$ was discussed very recently in Ref. [28]. There only lepton and quark loops have been considered. In the case of technipion production at the LHC we are rather interested in relatively large invariant diphoton masses $M_{\gamma\gamma} \gtrsim 100$ GeV relevant for the SM Higgs boson searches as well. In the present paper, we shall calculate both the QCD and QED contributions and compare them differentially as a function of diphoton invariant mass suggesting potentially measurable a signature of vector-like Technicolor.

II. TECHNIPION INTERACTIONS FROM VECTOR-LIKE TECHNICOLOR

We start from vector-like TC model setup relevant for our purposes here. The local chiral vector-like subgroup $SU(2)_{\rm V\equiv L+R} = SU(2)_{\rm W}$ appearing due to the spontaneous global chiral symmetry breaking (1.1) acts on confined elementary techniquark sector [23], i.e.

$$\tilde{Q} = \begin{pmatrix} U \\ D \end{pmatrix} , \tag{2.1}$$

which is thus in the fundamental representation of the SM gauge $SU(2)_{\rm W} \otimes U(1)_{\rm Y}$ group and $SU(3)_c$-neutral at the same time. As usual, in addition we have the initial scalar technisigma S field which is the SM singlet, and the triplet of initial (massless) technipion fields P_a, $a = 1, 2, 3$ which is the adjoint (vector) representation of $SU(2)_{\rm W}$ (with zeroth $U(1)_{\rm Y}$ hypercharge). The linear σ-model part of the Lagrangian responsible for the Yukawa-type interactions of the techniquarks (2.1) reads

$$\mathcal{L}_Y^{\rm TC} = -g_{\rm TC}\bar{\tilde{Q}}(S + i\gamma_5\tau_a P_a)\tilde{Q} \, , \tag{2.2}$$

where τ_a, $a = 1, 2, 3$ are the Pauli matrices, and effective Yukawa coupling $g_{\rm TC} > 1$. After the chiral and EW symmetries breaking, the Yukawa terms (2.2) determine the strength of technipion interactions with techniquarks as well as (pseudo)scalar self-couplings [23].

Non-local effects in gauge boson couplings to technipions and constituent techniquarks, in general, can be incorporated via momentum-dependent form factors. In the case of a large techniconfinement scale $\Lambda_{\rm TC} \sim 0.1 - 1$ TeV, these effects are strongly suppressed by large constituent masses of techniquarks $M_Q \sim \Lambda_{\rm TC}$ and can be neglected to the first approximation. Thus the vector-like gauge interactions of $\tilde{Q}$ and P_a fields with initial $U(1)_{\rm Y}$ and $SU(2)_{\rm W}$ gauge fields B_μ, W_μ^a, respectively, can be introduced in the local approximation via usual EW gauge couplings $g_{1,2}$ renormalized at the $\mu = 2M_Q$ scale, i.e.

$$\mathcal{L}_{\tilde{\pi},\tilde{Q}} = \frac{1}{2} D_\mu P_a \, D^\mu P_a + i\bar{\tilde{Q}}\hat{D}\tilde{Q} \, , \tag{2.3}$$

where

$$\hat{D}\tilde{Q} = \gamma^\mu \left(\partial_\mu - \frac{iY_Q}{2} g_1 B_\mu - \frac{i}{2} g_2 W_\mu^a \tau_a \right) \tilde{Q} \, , \tag{2.4}$$

$$D_\mu P_a = \partial_\mu P_a + g_2 \epsilon_{abc} W_\mu^b P_c \, ,$$

besides that $\tilde{Q}$ is also confined under a QCD-like $SU(N_{\rm TC})_{\rm TC}$ group. In this paper, we discuss a particular case with the number of technicolors $N_{\rm TC} = 3$.

After the EWSB, the physical Lagrangian of vector-like interactions of techniquarks and gauge bosons $V = Z^0$, $W^{\pm}$, γ reads

$$\begin{aligned} L_{\bar{\tilde{Q}}\tilde{Q}V} &= g_W^Q\, \bar{U}\gamma^\mu D \cdot W_\mu^+ + g_W^Q\, \bar{D}\gamma^\mu U \cdot W_\mu^- \\ &+ Z_\mu \sum_{Q=U,D} g_Z^Q\, \bar{f}\gamma^\mu f + \sum_{Q=U,D} g_\gamma^Q\, \bar{f}\gamma^\mu A_\mu f\,, \end{aligned} \tag{2.5}$$

where technifermion couplings to vector bosons $g_{V_{1,2}}^Q$ are

$$g_Z^Q = \frac{g}{c_W}\big(t_3^Q - q_Q s_W^2\big)\,, \quad g_W^Q = \frac{g}{\sqrt{2}}\,, \quad g_\gamma^Q = e\, q_Q\,. \tag{2.6}$$

Here, $s_W = \sin\theta_W$, $c_W = \cos\theta_W$, and θ_W is the Weinberg angle, $e = g s_W$ is the electron charge, t_3^Q is the weak isospin ($t_3^U = 1/2$, $t_3^D = -1/2$), $q_Q = Y_{\tilde{Q}}/2 + t_3^Q$ is the technifermion charge. Choosing the technifermion hypercharge to be the same as in the SM fermion sector $Y_{\tilde{Q}} = 1/3$, we get $q_U = 2/3$ and $q_D = -1/3$. Also, the Yukawa-type interactions of constituent techniquarks with technipions are governed by

$$L_{\bar{\tilde{Q}}\tilde{Q}\tilde{\pi}} = -i\sqrt{2} g_{\rm TC}\, \tilde{\pi}^+ \bar{U}\gamma_5 D - i\sqrt{2} g_{\rm TC}\, \tilde{\pi}^- \bar{D}\gamma_5 U - i g_{\rm TC}\, \tilde{\pi}^0 (\bar{U}\gamma_5 U - \bar{D}\gamma_5 D)\,. \tag{2.7}$$

Since we are interested here in neutral technipion couplings in exclusive production processes, only the last two terms of the Yukawa Lagrangian (2.7) will be used. Finally, Born-level interactions of technipions with gauge bosons are defined as follows

$$\begin{aligned} L_{\tilde{\pi}\tilde{\pi}V} &= i g_2 W^{\mu+} \cdot (\tilde{\pi}^0 \tilde{\pi}^-_{,\mu} - \tilde{\pi}^- \tilde{\pi}^0_{,\mu}) + i g_2 W^{\mu-} \cdot (\tilde{\pi}^+ \tilde{\pi}^0_{,\mu} - \tilde{\pi}^0 \tilde{\pi}^+_{,\mu}) \\ &+ i g_2 (c_W Z_\mu + s_W A_\mu) \cdot (\tilde{\pi}^- \tilde{\pi}^+_{,\mu} - \tilde{\pi}^+ \tilde{\pi}^-_{,\mu}) \\ &+ g_2^2\, W_\mu^+ W^{\mu-} \cdot (\tilde{\pi}^0 \tilde{\pi}^0 + \tilde{\pi}^+ \tilde{\pi}^-) + g_2^2\, (c_W Z_\mu + s_W A_\mu)^2 \cdot \tilde{\pi}^+ \tilde{\pi}^- + \ldots\,, \end{aligned} \tag{2.8}$$

where $\tilde{\pi}_{,\mu} \equiv \partial_\mu \tilde{\pi}$ notation is used for brevity. Other parts of the Lagrangian of the vector-like Technicolor model are not needed for present purposes and can be found in Refs. [23, 24].

It is worth to stress here that in distinction to extended TC scenarios, in the vector-like TC model the technipion interacts only with SM gauge bosons Z, γ and $W^{\pm}$ and with constituent $SU(3)_c$-singlet techniquarks. In practice, this makes the technipions rather difficult to produce and observe even in rather light ~ 100 GeV mass range.

III. TECHNIPION PRODUCTION AND DECAY: GAUGE BOSON CHANNELS

As it follows from Eq. (2.8), the pseudoscalar technipions can only be produced in pairs in gauge boson fusion reactions at Born level while single pion production is possible at one loop level only. For non-zeroth techniquark hypercharge $Y_Q \neq 0$, the effective one-loop technipion-vector bosons $\tilde{\pi}^0 V_1 V_2$ couplings are given by triangle diagrams shown in Fig. 1 (left). The latter is valid for the QCD-like TC scenario with $SU(3)_{\rm TC}$ group of confinement which is the subject of our analysis here. The corresponding loop amplitude has the following form

$$i\mathcal{V}_{\tilde{\pi}^0 V_1 V_2} = F_{V_1 V_2}(M_1^2, M_2^2, m_{\tilde{\pi}}^2; M_Q^2) \cdot \epsilon_{\mu\nu\rho\sigma} p_1^\mu p_2^\nu \varepsilon_1^{*\rho} \varepsilon_2^{*\sigma}\,, \tag{3.1}$$

$$F_{V_1 V_2} = \frac{N_{\rm TC}}{2\pi^2} \sum_{Q=U,D} g_{V_1}^Q\, g_{V_2}^Q\, g_{\tilde{\pi}^0}^Q\, M_Q\, C_0(M_1^2, M_2^2, m_{\tilde{\pi}}^2; M_Q^2)\,, \tag{3.2}$$

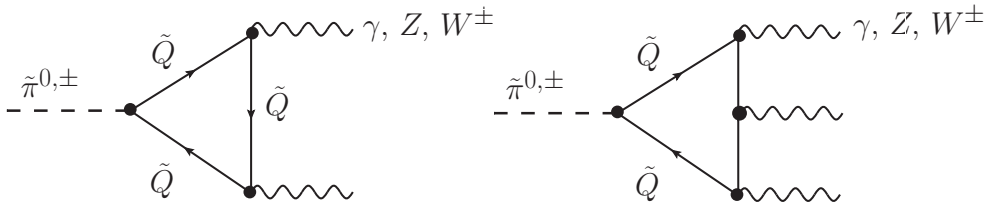

FIG. 1: The loop-induced light technipion couplings to the gauge bosons through constituent techniquark loops. In the case of $Y_Q \neq 0$, the technipion is coupled to two gauge bosons to the lowest order $\tilde{\pi}V_1V_2$ via techniquark triangle diagrams (left), while for the $Y_Q = 0$ case the technipion is coupled only to three gauge bosons $\tilde{\pi}V_1V_2V_3$ via a box diagram (right). The latter case is much more involved and will not be considered here.

where $C_0(m_1^2, m_2^2, m_3^2; m^2) \equiv C_0(m_1^2, m_2^2, m_3^2; m^2, m^2, m^2)$ is the standard finite three-point function, $N_{\rm TC}$ is the number of technicolors in confined $SU(N_{\rm TC})$ group, $p_{1,2}$, $\varepsilon_{1,2}$ and $M_{1,2}$ are the 4-momenta, polarization vectors of the vector bosons $V_{1,2}$ and their on-shell masses, respectively, and neutral technipion couplings to U, D techniquarks are

$$g^U_{\tilde{\pi}^0} = g_{\rm TC}\,, \quad g^D_{\tilde{\pi}^0} = -g_{\rm TC}\,, \tag{3.3}$$

while gauge couplings of techniquarks $g^Q_{V_{1,2}}$ are defined in Eq. (2.6). We have assumed $m_U = m_D = m_Q$. We should notice here that the $\tilde{\pi}^0 \to WW$ decay mode is forbidden by symmetry [23]. Finally, the explicit expressions of the effective neutral technipion couplings $F_{V_1V_2}$ for on-shell $V_1V_2 = \gamma\gamma$, γZ and ZZ final states are

$$F_{\gamma\gamma} = \frac{4\alpha\, g_{\rm TC}}{\pi}\frac{M_Q}{m^2_{\tilde{\pi}}}\,\arcsin^2\Big(\frac{m_{\tilde{\pi}}}{2M_Q}\Big)\,, \qquad \frac{m_{\tilde{\pi}}}{2M_Q} < 1\,, \tag{3.4}$$

$$F_{\gamma Z} = \frac{4\alpha\, g_{\rm TC}}{\pi}\frac{M_Q}{m^2_{\tilde{\pi}}}\,\cot 2\theta_W\,\Big[\arcsin^2\Big(\frac{m_{\tilde{\pi}}}{2M_{\tilde{Q}}}\Big) - \arcsin^2\Big(\frac{M_Z}{2M_{\tilde{Q}}}\Big)\Big]\,, \tag{3.5}$$

$$F_{ZZ} = \frac{2\alpha\, g_{\rm TC}}{\pi} M_Q\, C_0(M_Z^2, M_Z^2, m^2_{\tilde{\pi}}; M^2_{\tilde{Q}})\,, \tag{3.6}$$

where $\alpha = e^2/4\pi$ is the fine structure constant.

Now the two-body technipion decay width in a vector boson channel can be represented in terms of the effective couplings (3.2) as follows:

$$\Gamma(\tilde{\pi}^0 \to V_1\, V_2) = r_V \frac{m^3_{\tilde{\pi}}}{64\pi}\,\bar{\lambda}^3(M_1^2, M_2^2; m^2_{\tilde{\pi}})\,|F_{V_1V_2}|^2\,, \tag{3.7}$$

where $r_V = 1$ for identical bosons V_1 and V_2 and $r_V = 2$ for different ones, and $\bar{\lambda}$ is the normalized Källen function

$$\bar{\lambda}(m_a, m_b; q) = \Big(1 - 2\frac{m_a^2 + m_b^2}{q^2} + \frac{(m_a^2 - m_b^2)^2}{q^4}\Big)^{1/2}\,. \tag{3.8}$$

In Fig. 1 (right) we show the leading-order contribution to single technipion-gauge bosons coupling for $Y_Q = 0$ (relevant in the case of an even $SU(N_{\rm TC})_{\rm TC}$ group of confinement, e.g. $SU(2)_{\rm TC}$ [24]). In the latter case, a single technipion can be produced in V_1V_2 fusion only in association with an extra gauge boson V_3 while produced technipion should further decay either into three gauge bosons $\tilde{\pi} \to V_1'V_2'V_3'$ or into a pair of Higgs bosons $\tilde{\pi} \to hh$. Such processes would be rather suppressed and difficult to study experimentally while they give rise to the only observable signatures of technipions in the case of $SU(2)_{\rm TC}$ group of confinement in the vector-like Technicolor scenario so will be studied elsewhere.

IV. INCLUSIVE TECHNIPION PRODUCTION: THE VBF MECHANISM

Since technipions do not couple directly to SM fermions and gluons, the only way to produce them is in the vector-boson ($\gamma\gamma$, γZ, ZZ) fusion channel. The VBF is typically considered as one of the key production modes of the Higgs boson at the LHC which allowed recently for a clear discrimination of the Higgs signal [17, 18]. Corresponding typical partonic $2 \to 3$ hard subprocesses of Higgs boson and $\tilde{\pi}$ production in high energy hadron-hadron collisions via intermediate VBF mechanism are shown in Fig. 2. While VBF Higgs studies were properly done elsewhere [23], here we focus on the VBF into a neutral technipion only.

In Fig. 3 we show characteristic diagrams for the inclusive (left) and central exclusive (right) technipion production processes in dominant $\gamma\gamma$ fusion and decay channel. Both, production and decay subprocesses are initiated by triangle loop of U, D techniquarks. We

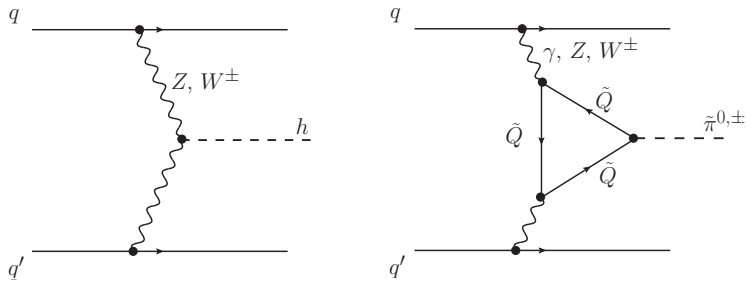

FIG. 2: Typical VBF production channels of the Higgs boson at tree level (left) and technipion via a triangle techniquark loop (right) via a gauge boson fusion in the quark-(anti)quark scattering.

assume $m_U = m_D$. Thus, the leading-order hard (parton level) VBF subprocess in the inclusive h (left) and $\tilde{\pi}$ (right) production in the high energy pp scattering is quark-initiated one

$$q_i q_j' \to q_i q_j' (\gamma^*\gamma^* \to h,\, \tilde{\pi}^0)\,, \tag{4.1}$$

where q_i and q_j can be either a quark or an antiquark of various flavors from each of the colliding protons, and the virtual $\gamma\gamma$ fusion is concerned. So, the both VBF processes, the h and $\tilde{\pi}^0$ production may "compete". While $h \to \gamma\gamma$ branching ratio is very small $\sim 10^{-3}$, the corresponding $\tilde{\pi}^0 \to \gamma\gamma$ one is fairly large ~ 1. On the other hand, the Higgs boson has additional dominating production modes e.g. via gluon-gluon fusion mechanism and the Higgsstrahlung off gauge bosons and heavy flavor. In contrast to the Higgs boson production, one technipion can be produced only via heavy techniquark triangle loop in the VBF mechanism. Such observable signatures similar to those of the Higgs boson open an interesting and straightforward opportunity for technipion searches in standard Higgs boson studies at the LHC.

The calculation of the inclusive production cross sections in QCD is rather straightforward and based upon standard collinear factorisation technique so we do not discuss it here. In numerical estimations of these cross sections which will be discussed later in the Results section, it is naturally assumed that the incoming quark q_i and (anti)quark q_j' loose only a small fraction of their initial energy taken away by intermediate vector bosons. In this kinematics, the final-state quarks are seen as forward-backward hard jets, and by measuring their momenta one accurately reconstructs the invariant mass of the produced state. As was advocated in Ref. [23], an overall one-technipion production rate is strongly suppressed

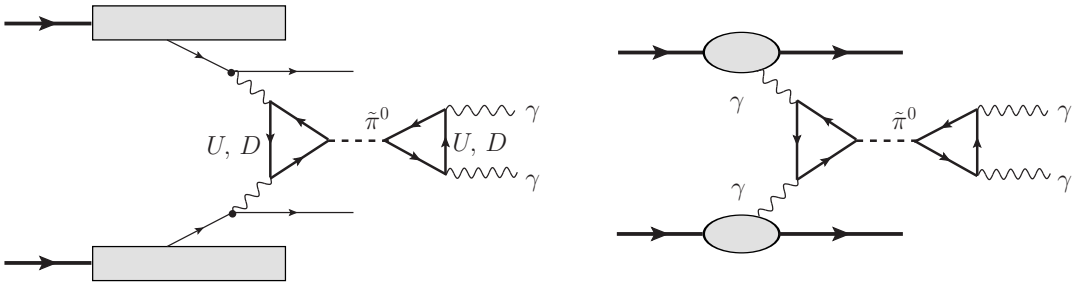

FIG. 3: Hadron-level technipion production channels in VBF mechanism and the leading $\gamma\gamma$ decay channel: inclusive $\tilde{\pi}^{0,\pm}$ production in association with two quark jets (left) and the central exclusive $\tilde{\pi}^0$ production in the $\gamma\gamma$ fusion (right).

compared to the Higgs boson production rate, which along with extremely narrow technipion resonance makes it rather hard to study experimentally. So, even light technipions down to W boson mass may be not excluded yet by LEP II and LHC studies, and the latter point is an interesting subject for further investigations.

V. EXCLUSIVE TECHNIPION PRODUCTION: THE VBF MECHANISM

Now we consider the central exclusive $pp \to pp\tilde{\pi}^0$ process illustrated in Fig. 3 (right). Similarly to the inclusive case discussed above, this process is determined by the colorless VBF subprocess. We take into account only for dominating $\gamma\gamma \to \tilde{\pi}^0$ fusion reaction and omit $\gamma Z \to \tilde{\pi}^0$, $Z\gamma \to \tilde{\pi}^0$ and $ZZ \to \tilde{\pi}^0$ subprocesses which turn out to be numerically very small being suppressed by large masses in propagators. The corresponding matrix element for the hadron-level $2 \to 3$ process can be written as:

$$\mathcal{M}^{pp\to pp\tilde{\pi}^0}_{\lambda_a\lambda_b\to\lambda_1\lambda_2} \;=\; V^{\mu_1}_{\lambda_a\to\lambda_1}\frac{(-ig_{\mu_1\nu_1})}{t_1}F_{\gamma\gamma}(M_Q,m_{\tilde{\pi}})\epsilon^{\nu_1\nu_2\alpha\beta}q_{1,\alpha}q_{2,\beta}\frac{(-ig_{\mu_2\nu_2})}{t_2}V^{\mu_2}_{\lambda_b\to\lambda_2}\,, \qquad (5.1)$$

where the parton-level triangle amplitude $F_{\gamma\gamma}(M_Q, m_{\tilde{\pi}})$ is given by Eq. (3.4), and the vertex functions $V_{\mu_{1,2}}$ can be approximated in the spin conserving case relevant at high energies as follows

$$V^{\mu_1}_{\lambda_a\to\lambda_1} \simeq F_1(t_1)\bar{u}(\lambda_1)i\gamma^{\mu_1}u(\lambda_a)\,, \quad V^{\mu_2}_{\lambda_b\to\lambda_2} \simeq F_1(t_2)\bar{u}(\lambda_2)i\gamma^{\mu_2}u(\lambda_b)\,, \qquad (5.2)$$

where $F_1(t)$ is the electromagnetic proton form factor. The natural limitation for a light pseudo-Goldstone technipion

$$\frac{m_{\tilde{\pi}}}{2M_Q} < 1 \qquad (5.3)$$

is implied. The matrix element specified above is used in a three-body calculation precisely as for the usual exclusive pion production in the $pp \to pp\pi^0$ process considered in Ref. [29].

VI. EXCLUSIVE $\gamma\gamma$ BACKGROUND: QCD VS QED MECHANISMS

In order to estimate the feasibility of exclusive technipion production studies we need to analyze carefully the exclusive $\gamma\gamma$ background. There are two basic non-resonant leading

order box-induced contributions – the QCD (Durham) diffractive mechanism via $gg \to \gamma\gamma$ shown in Fig. 4 (left) and the QED (light-by-light) scattering mechanism $\gamma\gamma \to \gamma\gamma$ shown in Fig. 4 (right). Below, we discuss both of them in detail.

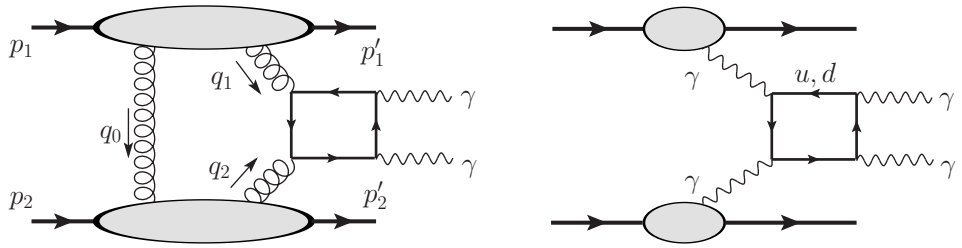

FIG. 4: Irreducible non-resonant background processes for the central exclusive technipion $\tilde{\pi}^0 \to \gamma\gamma$ production in pp collisions at the LHC: the QCD diffractive $\gamma\gamma$ pair production (left) and the QED-initiated $\gamma\gamma$ pair production (right). In the latter case, only a part of contributions corresponding to quark boxes is shown here for illustration while in actual calculations the full set of SM contributions including quark, lepton and W boson loops is taken into account.

A. Durham QCD mechanism

A schematic diagram for central exclusive production of $\gamma\gamma$ pairs in proton-proton scattering $pp \to p(\gamma\gamma)p$ with relevant kinematics notations is shown in Fig. 4 (left). In what follows, we use the standard theoretical description of CEP processes developed by the Durham group for the exclusive production of Higgs boson in Ref. [3]. The details of the kinematics for the central exclusive production processes can be found e.g. in Ref. [1]. Here we only sketch basic notations used in our calculations, which are similar to those in our previous paper on the central exclusive production of W^+W^- pairs [8].

The momenta of intermediate gluons are given by Sudakov decomposition in terms of the incoming proton four-momenta $p_{1,2}$

$$\begin{aligned} &q_1 = x_1 p_1 + q_{1\perp}, \quad q_2 = x_2 p_2 + q_{2\perp}, \quad 0 < x_{1,2} < 1, \\ &q_0 = x' p_1 - x' p_2 + q_{0\perp} \simeq q_{0\perp}, \quad x' \ll x_{1,2}, \end{aligned} \tag{6.1}$$

where $x_{1,2}, x'$ are the longitudinal momentum fractions for active (fusing) and color screening gluons, respectively, such that $q_\perp^2 \simeq -|\mathbf{q}_\perp|^{\mathbf{2}}$.

The QCD factorisation of the process at the hard scale μ_F is provided by the large invariant mass of the $\gamma\gamma$ pair $M_{\gamma\gamma}$, i.e.

$$\mu_F^2 \equiv s\, x_1 x_2 \simeq M_{\gamma\gamma}^2 \,. \tag{6.2}$$

It is convenient to introduce the Sudakov expansion for photon momenta as follows

$$k_3 = x_1^+ p_1 + x_2^+ p_2 + k_{3\perp}, \quad k_4 = x_1^- p_1 + x_2^- p_2 + k_{4\perp} \tag{6.3}$$

leading to

$$x_{1,2} = x_{1,2}^+ + x_{1,2}^-, \quad x_{1,2}^+ = \frac{|\boldsymbol{k}_{3,4\perp}|}{\sqrt{s}} e^{\pm y_3}, \quad x_{1,2}^- = \frac{|\boldsymbol{k}_{3,4\perp}|}{\sqrt{s}} e^{\pm y_4} \tag{6.4}$$

in terms of photon rapidities $y_\pm$ and transverse masses $m_{3,4\perp}$. For simplicity, in actual calculations we work in the forward limit which implies that $\boldsymbol{k}_{3\perp} \simeq -\boldsymbol{k}_{4\perp}$.

We write the amplitude of the diffractive process, which at high energy is dominated by its imaginary part, as

$$\mathcal{M}_{\lambda_3\lambda_4}(s,t_1,t_2) \;\simeq\; is\frac{\pi^2}{2}\int d^2\boldsymbol{q}_{0\perp} V_{\lambda_3\lambda_4}(q_1,q_2,k_3,k_4)\frac{f_g(q_0,q_1;t_1)f_g(q_0,q_2;t_2)}{\boldsymbol{q}_{0\perp}^2\,\boldsymbol{q}_{1\perp}^2\,\boldsymbol{q}_{2\perp}^2}\,, \qquad (6.5)$$

where $\lambda_{3,4} = \pm 1, 0$ are the polarisation states of the produced photons, respectively, $f_g(r_1,r_2;t)$ is the off-diagonal unintegrated gluon distribution function (UGDF), which depends on the longitudinal and transverse components of both gluon momenta. The gauge-invariant $gg \to \gamma_{\lambda_3}\gamma_{\lambda_4}$ hard subprocess amplitude $V_{\lambda_3\lambda_4}(q_1,q_2,k_3,k_4)$ is given by the light cone projection

$$V_{\lambda_3\lambda_4} = n_\mu^+ n_\nu^- V_{\lambda_3\lambda_4}^{\mu\nu} = \frac{4}{s}\frac{q_{1\perp}^\nu}{x_1}\frac{q_{2\perp}^\mu}{x_2}V_{\lambda_3\lambda_4,\mu\nu}, \quad q_1^\nu V_{\lambda_3\lambda_4,\mu\nu} = q_2^\mu V_{\lambda_3\lambda_4,\mu\nu} = 0\,, \qquad (6.6)$$

where $n_\mu^\pm = p_{1,2}^\mu/E_{p,cms}$ and the center-of-mass proton energy $E_{p,cms} = \sqrt{s}/2$. We adopt the definition of gluon polarisation vectors proportional to transverse momenta $q_{1,2\perp}$, i.e. $\epsilon_{1,2} \sim q_{1,2\perp}/x_{1,2}$. The helicity matrix element in the previous expression reads

$$V_{\lambda_3\lambda_4}^{\mu\nu}(q_1,q_2,k_3,k_4) = \varepsilon^\rho(k_3,\lambda_3)\varepsilon^\sigma(k_4,\lambda_4)V_{\rho\sigma}^{\mu\nu}\,, \qquad (6.7)$$

in terms of the Lorentz and gauge invariant $2 \to 2$ amplitude $V_{\rho\sigma}^{\mu\nu}$ and photons polarisation vectors $\varepsilon(k,\lambda)$. Below we will analyze the exclusive production with polarized photons. In Eq. (6.7) $\varepsilon_\mu(k_3,\lambda_3)$ and $\varepsilon_\nu(k_4,\lambda_4)$ can be defined easily in the proton-proton center-of-mass frame with z-axis along the proton beam as

$$\varepsilon(k,\pm 1) \;=\; \frac{1}{\sqrt{2}}\,(0,\; i\sin\phi \mp \cos\theta\cos\phi,\; -i\cos\phi \mp \cos\theta\sin\phi,\; \pm\sin\theta)\;, \qquad (6.8)$$

where ϕ is the azimuthal angle of a produced photon, and $\varepsilon^\mu(\lambda)\varepsilon_\mu^*(\lambda) = -1$ and $\varepsilon_\mu(k_3,\lambda_3)k_3^\mu = \varepsilon_\nu(k_4,\lambda_4)k_4^\nu = 0$. In the forward scattering limit, the azimuthal angles of the final state photons are related as $\phi_3 = \phi_4 + \pi$.

The diffractive amplitude given by Eq. (6.5) is averaged over the color indices and over the two transverse polarizations of the incoming gluons. The relevant color factor which includes summing over colors of quarks in the box loop and averaging over fusing gluon colors (according to the definition of unintegrated gluon distribution function) is the same as in the previously studied Higgs CEP [31] (for more details on derivation of the generic $pp \to pXp$ amplitude, see e.g. Ref. [1]). The matrix element V_{λ_3,λ_4} contains twice the strong coupling constant $g_s^2 = 4\pi\alpha_s$. In our calculation here we take the running coupling constant $\alpha_s(\mu_{\rm hard}^2 = M_{\gamma\gamma}^2)$ which depends on the invariant mass of $\gamma\gamma$ pair as a hard renormalisation scale of the process. The choice of the scale introduces roughly a factor of two uncertainty when varying the hard scale $\mu_{\rm hard}$ between $2M_{\gamma\gamma}$ and $M_{\gamma\gamma}/2$.

The bare amplitude above is subjected to absorption corrections that depend on the collision energy and typical proton transverse momenta. As was done in original Durham calculations [3], the bare production cross section is usually multiplied by a gap survival factor which we take the same as for the Higgs boson and $b\bar{b}$ production to be $S_g = 0.03$ at the LHC energy (see e.g. Ref. [30]).

The diffractive $\gamma\gamma$ CEP amplitude (6.5) described above is used now to calculate the corresponding cross section including realistic limitations on the phase space. For the sake of simplicity, assuming an exponential slope of $t_{1,2}$-dependence of the UGDFs [3], and as a consequence of the approximately exponential dependence of the cross section on t_1 and t_2 (proportional to $\exp(bt_1)$ and $\exp(bt_2)$), the four-body phase space can be calculated as

$$d\sigma \approx \frac{1}{2s}\overline{|\mathcal{M}|^2}\Big|_{t_{1,2}=0} \frac{1}{2^4}\frac{1}{(2\pi)^8}\frac{1}{E_1' E_2'}\frac{1}{4}\frac{1}{b^2}(2\pi)^2\frac{p_{m\perp}}{4}\mathcal{J}^{-1}\, dy_3 dy_4 dp_{m\perp} d\phi_m\,. \tag{6.9}$$

Since in this approximation we have assumed no correlations between outgoing protons (which is expected here and is practically true for the production of $b\bar{b}$ [31] or gg [30] dijets) there is no dependence of the integrand in Eq. (6.9) on ϕ_m, which means that the phase space integration can be further reduced to three-dimensional one. The Jacobian $\mathcal{J}$ in Eq. (6.9) is given by [32]

$$\mathcal{J} = \left| \frac{p_{1z}'}{\sqrt{m_p^2 + p_{1z}'^2}} - \frac{p_{2z}'}{\sqrt{m_p^2 + p_{2z}'^2}} \right|. \tag{6.10}$$

In actual calculations below we shall use the reduced form of the four-body phase space Eq. (6.9), and it is checked to give correct numerical results against the full phase space calculation for some simple reactions. Different representations of the phase space depending on a particular kinematical distributions needed can be found in Ref. [32].

Typical contributions to the leading order $gg \to \gamma\gamma$ subprocess are shown in Fig. 5. The total number of topologically different loop diagrams in the Standard Model amounts to twelve boxes. So the $\gamma\gamma$ background does not exhibit resonant features which is good for probing New Physics $\gamma\gamma$-resonant contributions like the technipion signal under consideration.

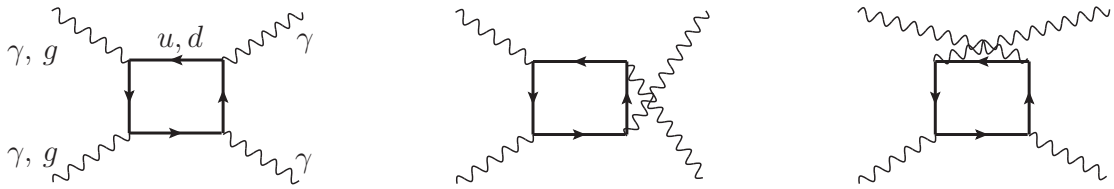

FIG. 5: Representative topologies of the hard subprocesses $gg \to \gamma\gamma$ and $\gamma\gamma \to \gamma\gamma$, which contribute to exclusive $\gamma\gamma$ pair production. These subprocesses constitute the irreducible background for the exclusive $\tilde{\pi}^0 \to \gamma\gamma$ reaction at the LHC. In the $gg \to \gamma\gamma$ case only quarks propagate in boxes and the amplitude is dominated by light quarks. In the $\gamma\gamma \to \gamma\gamma$ case, all the charged fermions – quarks, leptons, as well as $W^{\pm}$ bosons participate in the corresponding box diagrams. In the latter case, only a part of contributions corresponding to quark boxes is shown here for illustration.

The box contributions to the $gg \to \gamma\gamma$ parton level subprocess amplitude in Fig. 5 for on-shell fusing gluons were calculated analytically by using the Mathematica-based `FormCalc` (FC) [33] package. The complete matrix element was automatically generated by FC tools in terms of one-loop Passarino-Veltman two-, three- and four-point functions and other internally-defined functions (e.g. gluon and vector bosons polarisation vectors) and kinematical variables. In the next step, the Fortran code for the matrix element was generated, and then used as an external subroutine in our numerical calculations together with other

FC routines setting up the Standard Model parameters, coupling constants and kinematics. Instead of built-in FC polarisation vectors we have used transverse gluon polarisation vectors which enter the projection in Eq. (6.6), and the standard photon polarisation vectors defined in Eq. (6.8), giving an access to individual polarisation states of the photons. In accordance with the k_t-factorisation technique, the gauge invariance of the resulting amplitudes for the on-mass-shell initial gluons is ensured by a projection onto the gluon transverse polarisation vectors proportional to the transverse gluon momenta $q_{1,2\perp}$ according to Eq. (6.6).

For the evaluation of the scalar master tree- and four-point integrals in the gluon-gluon fusion subprocess we have used the `LoopTools` library [33]. The result is summed up over all possible quark flavors in loops and over distinct loop topologies. We have also checked that the sum of relevant diagrams is explicitly finite and obeys correct asymptotical properties and energy dependence. It is worth to mention that a large cancelation between separate box contributions in the total sum of diagrams takes place, which is expected from the general Standard Model symmetry principles.

As soon as the hard subprocess matrix element (denoted above as $V_{\lambda_3\lambda_4}$) has been defined as a function of relevant kinematical variables (four-momenta of incoming/outgoing particles), the loop integration over $q_{0\perp}$ in Eq. (6.5) was performed to obtain the diffractive amplitude, which then has been used to calculate the differential distributions for (un)polarised photon in an external phase space integrator.

B. QED-initiated $\gamma\gamma \to \gamma\gamma$ reaction

In this subsection, we briefly discuss the mechanism of exclusive production of two photons via hard $\gamma\gamma \to \gamma\gamma$ subprocess as illustrated in Fig. 4 (left).

The light-by-light $\gamma\gamma \to \gamma\gamma$ scattering subprocess to the leading and next-to-leading order was discussed earlier in the literature (see e.g. Refs. [34, 35]). The relevant subprocess diagrams are similar in topology to those for $gg \to \gamma\gamma$ shown in Fig. 5 but contain extra contributions from leptonic and vector boson W loops. The next-to-leading order corrections [35] were found to be rather small. So in the present paper with the focus on $pp \to pp\gamma\gamma$ process we consider the leading-order approximation for the $\gamma\gamma \to \gamma\gamma$ subprocess only.

The cross section of exclusive $\gamma\gamma$ production in pp scattering can be calculated in the same way as in the parton model in the so-called equivalent photon approximation as

$$\frac{d\sigma}{dy_3 dy_4 d^2p_{\gamma\perp}} = \frac{1}{16\pi^2\hat{s}^2} x_1\gamma(x_1) x_2\gamma(x_2) \overline{|\mathcal{M}_{\gamma\gamma\to\gamma\gamma}(\lambda_1,\lambda_2,\lambda_3,\lambda_4)|^2} \,. \tag{6.11}$$

A more involved and precise four-body calculation for the $pp \to pp\gamma\gamma$ is expected to give a very similar result [8].

In the parton formula above, $\gamma(x)$ is an elastic flux (x-distribution) of equivalent photons associated with elastic electromagnetic emission off a proton. In practical calculations we shall use parametrization proposed in Ref. [36]. In the same way as for QCD diffractive mechanism described above, the loop-induced helicity matrix elements for the $\gamma\gamma \to \gamma\gamma$ subprocess were calculated by using `LoopTools` [33]. In numerical calculations we include box diagrams with lepton, quark as well as with W bosons. At high diphoton invariant masses the inclusion of diagrams with W bosons is crucial. In principle, effects beyond the Standard Model possibly responsible for anomalous gauge couplings could be important [34, 37–40], so the exclusive non-resonant $\gamma\gamma$ background is very interesting by itself. In the

present analysis we concentrate on the search for technipion so we ignore effects beyond the Standard Model as far as the background is considered.

VII. RESULTS

Before discussing results for exclusive production of neutral technipion, we would like to summarize the inclusive $\tilde{\pi}^0$ production in association with two forward jets. In Fig. 6 we show the total inclusive cross section as a function of technipion (left) and techniquark (right) masses, $m_{\tilde{\pi}}$ and $M_{\tilde{Q}}$, respectively, and integrated over the full phase space. The

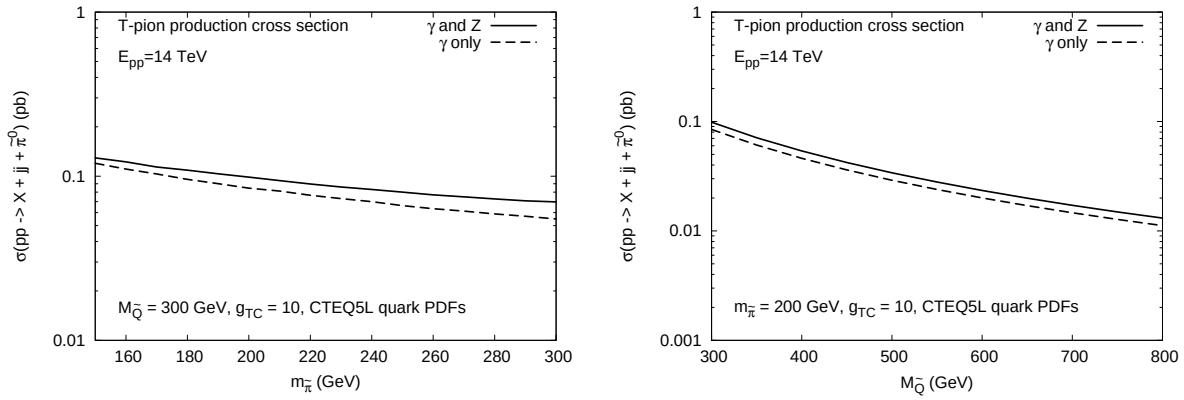

FIG. 6: Inclusive $\tilde{\pi}^0$ production cross section in association with two forward jets as a function of technipion mass (left panel) and as a function of techniquark mass (right panel) for fixed values of the g_{tc} coupling constant at the nominal LHC energy $\sqrt{s} = 14$ TeV.

calculation was performed in the collinear QCD factorization with hard (parton-level) $2 \to 3$ subprocess (4.1) including t-channel exchanges of γ and Z^0 bosons as illustrated in Fig. 3 (left) (for more details we refer to Ref. [23]). This calculation includes all the light quark and antiquark flavors in the initial state with respective quark PDFs. As can be seen from Fig. 6 the photon-photon $\gamma\gamma$ fusion mechanism dominates, while $Z\gamma$ and ZZ fusion contributions are always small (suppressed by a large mass of Z boson in propagators). The cross section for the vector-like TC model parameters and CTEQ5L quark PDFs [41] chosen as indicated in the figure is of the order of 100 fb.

Now let us look into the parameter dependence of the exclusive production cross section. This calculation is performed in the same way as the calculation for the exclusive production of usual pion π^0 studied recently by two of us in Ref. [29]. In particular, Fig. 7 shows a 2D map of the full phase space integrated cross section as a function of technipion and techniquark masses. A kinematical limit $m_{\tilde{\pi}} = 2M_{\tilde{Q}}$ is clearly visible. We obtain the cross section of the order of 1 fb for the same parameters as used in the calculation of the inclusive cross section. This is about two orders of magnitude less than in the inclusive case. The signal-to-background ratio, as will be discussed later is, however, more advantageous in the exclusive case than in the inclusive one.

In Fig. 8 we show one-dimensional dependencies on technipion (left) and techniquark (middle) masses. These dependencies can be compared to those in Fig. 6. Finally in Fig. 8 (right) we show dependence on technipion mass for fixed ratio of techniquark-to-technipion

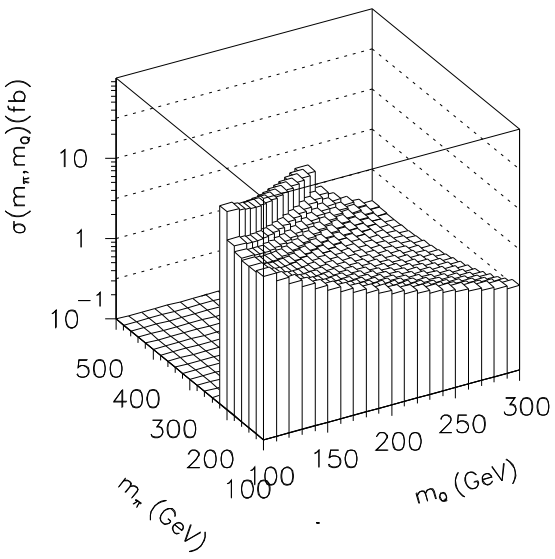

FIG. 7: Exclusive cross section as a 2D function of technipion mass ($m_{\tilde{\pi}}$) and techniquark mass ($M_{\tilde{Q}}$) for a fixed value of $g_{\rm TC} = 10$.

mass ratio. The latter dependence looks, however, steeper as an artifact of parameter correlations.

In the exclusive case, the integration in proton transverse momenta requires a special care. Instead of integration over $p_{1\perp}$ and $p_{2\perp}$ we integrate over: $\xi_1 = \log_{10}(p_{1\perp}/1\,\text{GeV})$ and $\xi_2 = \log_{10}(p_{2\perp}/1\,\text{GeV})$. The resulting cross section in the auxiliary quantities is shown in Fig. 9.

Now let us consider some important differential distributions. In Fig. 10 we show a distribution in technipion rapidity (left panel) and azimuthal angle between outgoing protons (right panel). The larger the technipion mass the smaller the cross section. The technipions are produced dominantly at midrapidities as expected.

Up to now we have discussed cross sections and differential distributions for technipion

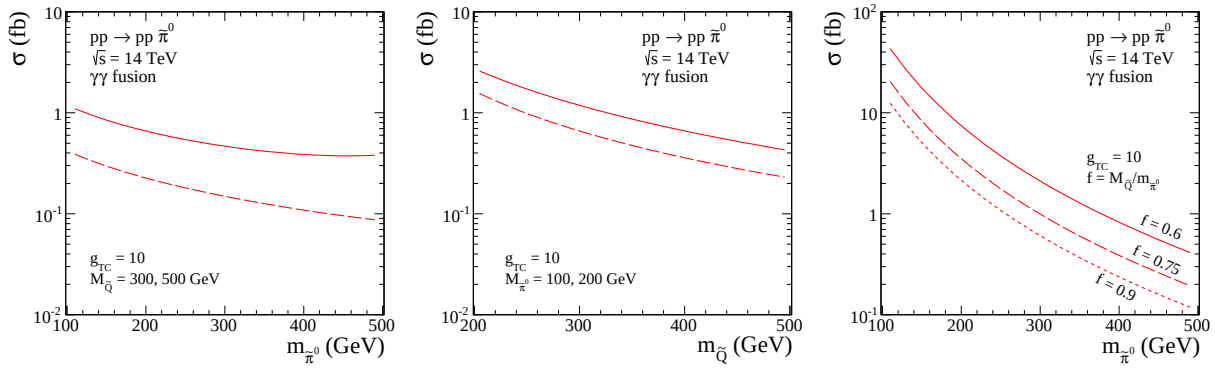

FIG. 8: Integrated exclusive cross section as a function of technipion mass (left) and techniquark mass (middle) for fixed remaining model parameters as specified in the figure. In the right panel we show the cross section as a function of technipion mass for a few fixed ratios $f = M_{\tilde{Q}}/m_{\tilde{\pi}}$.

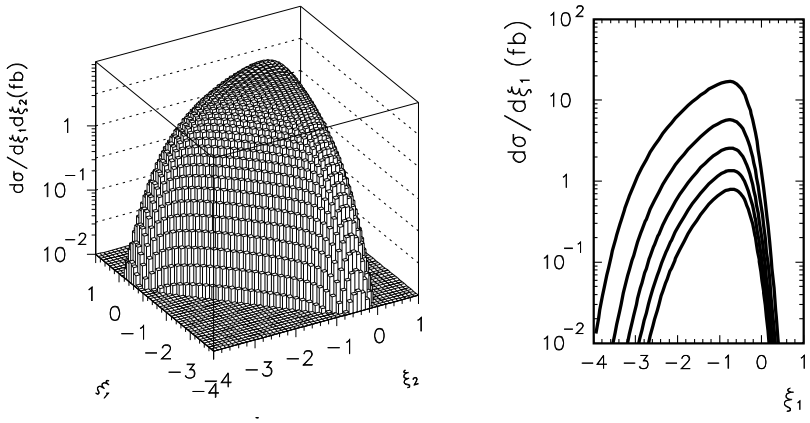

FIG. 9: Two-dimensional distribution in the auxiliary quantities $\xi_1 = log_{10}(p_{1t}/1\text{GeV})$ and $\xi_2 = log_{10}(p_{2t}/1\text{GeV})$ (left) and the projection on one of the axes (right).

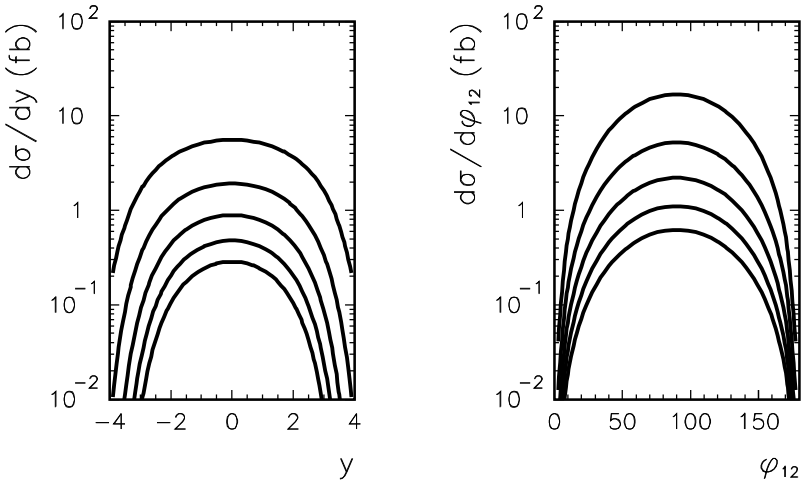

FIG. 10: Differential distributions in technipion rapidity (left panel) and azimuthal angle between outgoing protons (right panel) for different masses of the technipion ($m_{\tilde{\pi}} = 100$, 200, 300, 400, 500 GeV from top to bottom). The techniquark mass is fixed to be $M_{\tilde{Q}} = 0.75 m_{\tilde{\pi}}$.

production in exclusive pp scattering. In real experiment, an optimal decay channel must be chosen due to presumably low production cross sections, on the one hand, and to maximize the signal-to-background ratio, on the other hand. In Fig. 11 we show branching fractions for major real technipion $\tilde{\pi}^0$ decay channels. In a very broad range of technipion and techniquark masses the two-photon decay channel seems to be the most optimal one. In addition, this is one of the golden channels for Higgs boson searches and the LHC detectors are well suited for such studies.

Let us concentrate now on the exclusive diphoton background to the exclusive technipion production. In Fig. 12 we show the corresponding distribution in invariant mass of the two outgoing photons $M_{\gamma\gamma}$. We show distributions for the Durham QCD mechanism and

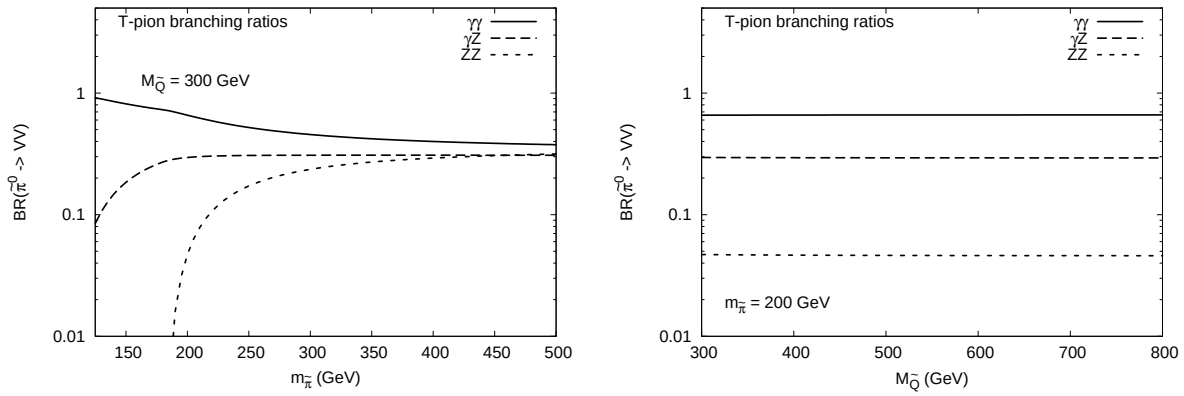

FIG. 11: Branching fractions of technipion decays into $\gamma\gamma$, γZ and ZZ final states as a function of technipion mass $m_{\tilde{\pi}}$ for a fixed value of techniquark mass (left) and as a function of techniquark mass $M_{\tilde{Q}}$ for a fixed value of technipion mass (right).

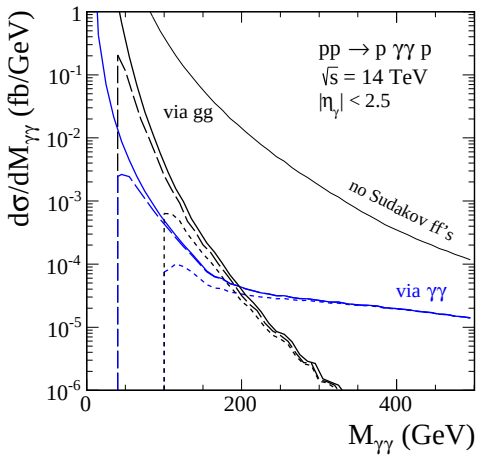

FIG. 12: Distribution in invariant mass of the two-photon system for the Durham QCD mechanism (black lines) and QED $\gamma\gamma$ fusion mechanism (blue lines). We present results without cuts (solid line) and with extra cuts on photon transverse momenta $p_{\perp,\gamma} > 20$, 50 GeV (long dashed, dashed lines, respectively) were imposed for illustration.

for the QED $\gamma\gamma$ fusion mechanism calculated based upon the parton-model formula (6.11). At relatively low masses, the Durham mechanism dominates. However, above $M_{\gamma\gamma} > 200$ GeV the photon-photon mechanism takes over. The later is therefore the most important potential background for the technipion signal if observed in the $\gamma\gamma$ decay channel. For the pQCD background we have also shown a result without Sudakov formfactors. As can bee seen from the figure the Sudakov formfactors strongly damp the cross section, especially at larger photon-photon invariant masses. Assuming the experimental resolution in invariant $\gamma\gamma$ mass of about 5 GeV or so, the background turns out to be by two orders of magnitude smaller than the corresponding technipion signal for the whole range of vector-like TC model parameters considered in the present paper. To summarize, the signal-to-background ratio in exclusive technipion production process is by far better than that in inclusive technipion production [23]. The latter is clear from comparing the corresponding inclusive $\gamma\gamma$ back-

TABLE I: The cross sections (in fb) for photon-pair central exclusive production at $\sqrt{s} = 14$ TeV in the photon pseudorapidity $|\eta_\gamma| < 2.5$ and with cuts in $p_{\perp,\gamma} > 50$ GeV on both outgoing photons. Different choices of gluon PDF are used at quite small values of gluon transverse momenta $q^2_{\perp,min} = 0.5$ GeV^2.

$M_{\gamma\gamma}$	σ (fb) at $\sqrt{s} = 14$ TeV and $\|\eta_\gamma\| < 2.5$					
	$\gamma\gamma \to \gamma\gamma$		$gg \to \gamma\gamma$, GJR08VFNS NLO		$gg \to \gamma\gamma$, MSTW08 NLO	
	no cuts $p_{\perp,\gamma}$	$p_{\perp,\gamma} > 50$ GeV	no cuts $p_{\perp,\gamma}$	$p_{\perp,\gamma} > 50$ GeV	no cuts $p_{\perp,\gamma}$	$p_{\perp,\gamma} > 50$ GeV
50 – 100	97.01×10^{-3}	–	3.048	–	2.752	–
100 – 150	11.62×10^{-3}	4.10×10^{-3}	62.72×10^{-3}	22.55×10^{-3}	67.08×10^{-3}	23.20×10^{-3}
150 – 200	2.96×10^{-3}	2.01×10^{-3}	5.90×10^{-3}	4.21×10^{-3}	6.84×10^{-3}	4.74×10^{-3}
200 – 250	1.78×10^{-3}	1.51×10^{-3}	0.95×10^{-3}	0.79×10^{-3}	1.15×10^{-3}	0.94×10^{-3}
250 – 300	1.44×10^{-3}	1.34×10^{-3}	0.23×10^{-3}	0.21×10^{-3}	0.29×10^{-3}	0.25×10^{-3}
300 – 350	1.23×10^{-3}	1.19×10^{-3}	0.06×10^{-3}	0.05×10^{-3}	0.07×10^{-3}	0.07×10^{-3}
350 – 400	1.06×10^{-3}	1.05×10^{-3}	0.02×10^{-3}	0.02×10^{-3}	0.03×10^{-3}	0.02×10^{-3}

ground estimates which have been done earlier in the Higgs boson $\gamma\gamma$ signal studies at the LHC [17, 18] and typical inclusive technipion production cross sections shown e.g. in Fig. 6.

In Table I we list the total $pp \to p(\gamma\gamma)p$ exclusive cross sections at the LHC ($\sqrt{s} = 14$ TeV) for the QCD $gg \to \gamma\gamma$ and QED $\gamma\gamma \to \gamma\gamma$ mechanisms in separate 50 GeV - windows in diphoton $\gamma\gamma$ invariant mass $M_{\gamma\gamma}$ placed between 50 and 400 GeV of diphoton invariant mass. A realistic cut on both photon pseudorapidities $|\eta_\gamma| < 2.5$ is imposed. For comparison, we show the numerical results with an extra cut on transverse momenta of both outgoing photons $p_{\perp,\gamma} > 50$ GeV and without it, as well as for two different choices of the gluon PDFs [42, 43] entering the calculation of UGDF in the Durham approach (c.f. Eq. (6.5)). As we have already observed in Fig. 12, the QCD component of the exclusive $\gamma\gamma$ background dominates only for smaller invariant masses $M_{\gamma\gamma} \lesssim 200$ GeV, while for larger ones the QED mechanism becomes important. Observation of much larger cross section in only one of the windows than those given in Table 1 would be then a probable signal of a new resonance (technipion). On the other hand, observation of much larger cross section in many windows simultaneously would be a signal of new particles appearing in loops.

VIII. SUMMARY AND CONCLUSION

We have made a first analysis of an interesting possibility to search for technipions mostly decaying into two photons in exclusive $pp \to pp\gamma\gamma$ process at the LHC. We have considered a particularly interesting case of light technipions which do not directly interact with gluons and quarks to the leading order, but can interact only with SM gauge bosons. A single technipion in this case can only be produced via a techniquark triangle loop in a vector boson fusion channel. The latter specific properties of physical technipions are predicted, in particular, by recently suggested phenomenologically consistent vector-like Technicolor (TC) model [23]. We have calculated the dependence of the $pp \to pp\tilde{\pi}^0$ cross section on the vector-like TC model parameters. With a natural choice of parameters obtained by a mere QCD rescaling the corresponding cross sections of the order of one to a few femtobarns could be expected. This means that the exclusive $\tilde{\pi}^0$ production cross section can be of the same order or even exceeds the traditional Higgs boson CEP cross section [3, 31] making

the considered proposal very important for the forward physics program at the LHC [1, 2].

In the present analysis we have considered only purely exclusive process, i.e. we have assumed that the both outgoing protons are detected. This is not yet possible at the LHC, but could be possible when forward proton detectors are installed by the ATLAS and/or CMS collaborations.

We have calculated several differential distributions and discussed their characteristic features. The particularly interesting ones are distributions in azimuthal angle between outgoing protons. The outgoing protons are scattered dominantly to perpendicular azimuthal directions.

We have demonstrated that for not too large technipion masses the photon-photon decay channel has the largest branching fraction. This shows that the exclusive reaction $pp \to pp\gamma\gamma$ is probably the best suited in searches for technipions at the LHC.

We have therefore studied the expected Standard Model exclusive $\gamma\gamma$ backgrounds. We have considered two important sources of the non-resonant background: the Durham QCD mechanism (via $gg \to \gamma\gamma$ subprocess) and the QED mechanism (via $\gamma\gamma \to \gamma\gamma$ subprocess). In the later case we have included full set of box diagrams with lepton, quark and W boson loops thus focusing on the dominant Standard Model processes only. The most interesting is the distribution in diphoton invariant mass. At lower invariant masses, the Durham QCD mechanism dominates. At larger invariant masses, the light-by-light rescattering occurs to be more relevant background in searches for technipions. We conclude that the signal-to-background ratio would be very favorable in the reaction under consideration.

The light-by-light rescattering subprocess contribution to the exclusive diphoton signal at the LHC in large diphoton invariant masses is interesting in its own right as a good probe in searches for effects beyond the Standard Model (e.g. supersymmetry, Dirac monopoles etc). All this makes the $pp \to pp\gamma\gamma$ reaction particularly interesting for LHC phenomenology.

In the present analysis we have considered purely exclusive processes. The related experiments would require therefore measurements of forward protons. We hope this will be possible in a close future [2]. In principle, one could also allow semi-exclusive (e.g. single diffractive) processes when excited states of proton (proton resonances or continuum) are produced while the pile-up problem has to be solve in high luminosity runs. The latter will be investigated elsewhere.

Acknowledgments

Stimulating discussions and helpful correspondence with Johan Bijnens, Vitaly Beylin, Vladimir Kuksa, Johan Rathsman, Francesco Sannino, Torbjörn Sjöstrand and Grigory Vereshkov are gratefully acknowledged. This work was supported by the Crafoord Foundation (Grant No. 20120520) and by the Polish MNiSW grant DEC-2011/01/B/ST2/04535. R. P. is grateful to the "Beyond the LHC" Program at Nordita (Stockholm) for support and hospitality during initial stages of this work.

[1] M. G. Albrow, T. D. Coughlin and J. R. Forshaw, Prog. Part. Nucl. Phys. **65** (2010) 149.

[2] M. G. Albrow *et al.* [FP420 R&D Collaboration], JINST **4**, T10001 (2009).

[3] V. A. Khoze, A. D. Martin and M. G. Ryskin, Phys. Lett. **B401** (1997) 330; Eur. Phys. J. **C14** (2000) 525; Eur. Phys. J. **C19** (2001) 477 [Erratum-ibid. **C20** (2001) 599]; Eur. Phys.

J. **C23** (2002) 311;
A. B. Kaidalov, V. A. Khoze, A. D. Martin and M. G. Ryskin, Eur. Phys. J. **C33** (2004) 261.
[4] A. Dechambre, O. Kepka, C. Royon and R. Staszewski, Phys. Rev. **D83** (2011) 054013.
[5] M. G. Ryskin, A. D. Martin, V. A. Khoze, Eur. Phys. J. **C60** (2009) 265.
[6] R. S. Pasechnik, A. Szczurek and O. V. Teryaev, Phys. Rev. D **78**, 014007 (2008);
P. Lebiedowicz, R. Pasechnik and A. Szczurek, Phys. Lett. B **701**, 434 (2011).
[7] L. A. Harland-Lang, V. A. Khoze, M. G. Ryskin and W. J. Stirling, Eur. Phys. J. **C69** (2010) 179.
[8] P. Lebiedowicz, R. Pasechnik and A. Szczurek, Nucl. Phys. B **867**, 61 (2013).
[9] A. Szczurek, R. S. Pasechnik and O. V. Teryaev, Phys. Rev. **D75** (2007) 054021.
[10] L. A. Harland-Lang, V. A. Khoze, M. G. Ryskin and W. J. Stirling, Eur. Phys. J. **C71** (2011) 1714.
[11] R. Enberg and R. Pasechnik, Phys. Rev. **D83**, 095020 (2011).
[12] CMS Collaboration, CMS-PAS-HIG-13-016, 2013.
[13] S. Weinberg, Phys. Rev. **D13**, 974 (1976);
L. Susskind, Phys. Rev. **D20**, 2619 (1979).
[14] S. Dimopoulos and L. Susskind, Nucl. Phys. **B155**, 237 (1979);
E. Eichten and K. D. Lane, Phys. Lett. **B90**, 125 (1980).
[15] C. T. Hill and E. H. Simmons, Phys. Rept. **381**, 235 (2003) [Erratum-ibid. **390**, 553 (2004)] [hep-ph/0203079].
[16] F. Sannino, Acta Phys. Polon. B **40**, 3533 (2009).
[17] G. Aad *et al.* [ATLAS Collaboration], Phys. Lett. **B716**, 1 (2012); Science **338**, 1576 (2012).
[18] S. Chatrchyan *et al.* [CMS Collaboration], Phys. Lett. **B716**, 30 (2012); Science **338**, 1569 (2012).
[19] R. S. Chivukula, P. Ittisamai, E. H. Simmons and J. Ren, Phys. Rev. D **84**, 115025 (2011) [Erratum-ibid. D **85**, 119903 (2012)].
[20] J. Jia, S. Matsuzaki and K. Yamawaki, Phys. Rev. D **87**, 016006 (2013).
[21] M. T. Frandsen and F. Sannino, arXiv:1203.3988 [hep-ph].
[22] T. Hapola, F. Mescia, M. Nardecchia and F. Sannino, Eur. Phys. J. C **72**, 2063 (2012).
[23] R. Pasechnik, V. Beylin, V. Kuksa and G. Vereshkov, arXiv:1304.2081 [hep-ph].
[24] R. Pasechnik, V. Beylin, V. Kuksa and G. Vereshkov, arXiv:1308.6625 [hep-ph].
[25] B.W. Lee and H.T. Nieh, Phys. Rev. **166**, 1507 (1968).
[26] S. Gasiorowicz and D. Geffen, Rev. Mod. Phys. **41**, 531 (1969);
P. Ko and S. Rudaz, Phys. Rev. **D 50**, 6877 (1994);
M. Urban, M. Buballa, and J. Wambach, Nucl. Phys. **A697**, 338 (2002).
[27] B.D. Serot and J.D. Walecka, Acta Phys. Pol. **B21**, 655 (1992).
[28] D. d'Enterria and G. G. da Silveira, Phys. Rev. Lett. **111**, 080405 (2013).
[29] P. Lebiedowicz and A. Szczurek, Phys. Rev. **D87**, 074037 (2013).
[30] R. Maciuła, R. Pasechnik and A. Szczurek, Phys. Rev. **D84** 114014 (2011).
[31] R. Maciula, R. Pasechnik and A. Szczurek, Phys. Rev. **D82**, 114011 (2010);
Phys. Rev. **D83**, 114034 (2011).
[32] P. Lebiedowicz and A. Szczurek, Phys. Rev. **D81**, 036003 (2010).
[33] T. Hahn, Comput. Phys. Commun. **140**, 418 (2001);
T. Hahn and M. Perez-Victoria, Comput. Phys. Commun. **118**, 153 (1999);
T. Hahn, Comput. Phys. Commun. **178**, 217 (2008).
[34] G. Jikia and A. Tkabladze, Phys. Lett. B **323**, 453 (1994);

G. J. Gounaris, P. I. Porfyriadis and F. M. Renard, Eur. Phys. J. **C9**, 673 (1999); Phys. Lett. B **452**, 76 (1999) [Erratum-ibid. B **513**, 431 (2001)].
[35] Z. Bern, A. De Freitas, L. J. Dixon, A. Ghinculov and H. L. Wong, JHEP **0111**, 031 (2001).
[36] M. Drees and D. Zeppenfeld, Phys. Rev. **D39**, 2536 (1989).
[37] J. Ohnemus, T. F. Walsh and P. M. Zerwas, Phys. Lett. **B328**, 369 (1994).
[38] I. F. Ginzburg and A. Schiller, Phys. Rev. **D57**, 6599 (1998).
[39] H. Davoudiasi, Phys. Rev. **D60**, 084022 (1999).
[40] K.-M. Cheung, Phys. Rev. **D61**, 015005 (2000).
[41] H. L. Lai *et al.* [CTEQ Collaboration], Eur. Phys. J. C **12**, 375 (2000).
[42] M. Glück, P. Jimenez-Delgado, E. Reya, Phys. Lett. **B664** 133 (2008).
[43] A.D. Martin, W.J. Stirling, R.S. Thorne, G. Watt, Eur. Phys. J. **C63** 182 (2009).